EUV MODELS OF THE CHROMOSPHERE-CORONA TRANSITION REGION

Nirupama Raghavan

II / 33, *Indian Institute of Technology Campus*
New Delhi 110029

INTRODUCTION:

The chromosphere-corona transition region is a region of crucial importance for understanding the structure of the solar atmosphere. The intensity distribution of the solar continuum radiation is such, that at radio and optical wavelengths it is not particularly sensitive to temperature. Consequently, these radiations are not helpful in studying the transition region, whose outstanding characteristic is the sharp rise in temperature. Forbidden lines in the visible originate at temperatures typical of the transition region; however, the low transition probability coupled with a small emitting volume makes the lines too faint to be observed accurately against the optical continuum.

For the permitted resonance lines in the extreme ultraviolet, the situation becomes favourable because the continuum is weakened greatly. With the advent of the ability to make solar observations from space therefore, it has become possible to focus attention on the transition region.

FIRST MODELS:

First generation results are from intensities integrated over the entire disk. The transition region can be considered effectively thin and the globally averaged energy flux emitted by an area 1 cm^2 due to a transition from level 2 to level 1 of an ion is given by

$$F = 0.55 \times 10^{-15}\ gf\ A \int n_e^2\ G(T_e)\ dh, \quad (1)$$

where $G(T_e) = n_1\ T_e^{-1/2}\ \chi^{-1} \exp(-11600\ \chi / T_e)$.

Here g is the Gaunt factor, f is the oscillator strength, A is the abundance of the element relative to hydrogen, n_e is the electron density, n_1 the population of level 1 and χ the excitation potential. $G(T_e)$ is a known peaked function of temperature and can be replaced by $0.7G(T_{max})$. Thus

$$F = 0.385 \times 10^{-15}\ gf\ A\ G(T_{max}) \int_{\Delta T_e} n_e^2\ dh, \quad (2)$$

where ΔT_e gives the temperature range obtained through the normalization

$$\Delta T_e \langle G(T_e) \rangle = \int G(T_e)\ dT_e.$$

Thus, for any given element, the intensities of lines from different stages of ionization give $\int n_e^2\ dh$, as a function of temperature. Since the emission measure versus temperature curve should be unique, shifting the curve due to one element to match with that of another, at constant temperature, gives the relative abundances of the two elements. Thus Pottasch (1964) derived both relative abundances and the emission measures from observed fluxes.

The global flux equation can also be rewritten to get the temperature gradient, instead of the emission measure. Assuming that the scaled pressure $p = n_e T_e$ is constant over the transition region,

$$F = 0.55 \times 10^{-15}\ gf\ A\ p^2 \left\langle \left(\frac{dT_e}{dh} \right)^{-1} \right\rangle \times \int G(T_e)\ T_e^{-1/2}\ dT_e\ . \quad (3)$$

Observed fluxes can therefore be used to derive the temperature gradient of an atmosphere of known chemical abundance. Athay (1966), and Dupree and Goldberg (1967) showed that the temperature gradients so derived were consistent with an atmosphere in which

$$T_e^{5/2} \frac{dT_e}{dh} = \text{constant},$$

in the temperature range 10^5 to 10^6 K—that is, the downward conductive flux is approximately constant in this region. Observed global fluxes gave a value of 1.1×10^6 ergs $cm^{-2}\ s^{-1}$ for this flux. The high value of the conductive flux makes it the dominant energy flux in this region and its near constancy is in fact a consequence of its being large compared to other forms of energy flux. Fig. 1 shows the approximate temperature profile of the transition region and the low corona as obtained from integrated disk intensities.

SECOND GENERATION MODELS:

Observations over the last five years preceding the Apollo Telescope Mount (ATM) experiment have been either of modest spectral and spatial resolution and wide coverage (OSO 4 and 6) or of high spectral and spatial resolution over restricted regions (rocket studies of Culham and Naval Research Laboratory groups). Intensities have been observed (1) at a fixed position on or off the disk, as a function of wavelength and (2) through spectroheliograms where the intensity at one wavelength has been obtained as a function of position on the disk.

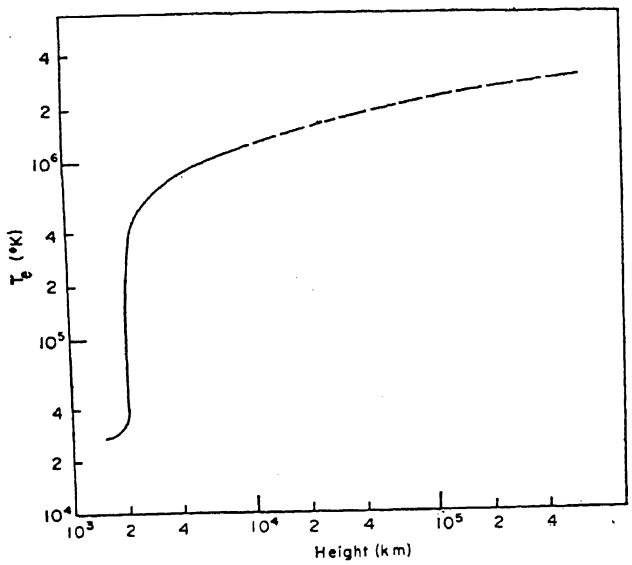

Fig. 1: Temperature—height profile of the chromosphere-corona transition region and the low corona (After Dupree and Goldberg (1967), courtesy Solar Physics).

The models derived from rocket studies refer to conditions at specific locations and at specific times. The Orbiting Solar Observatory observations have yielded a description of the conditions in the average quiet transition region and "average active" transition region. In what follows, these "average" descriptions would be considered in detail.

In order to derive an acceptable model of the transition region from the observed intensities, a set of assumptions are needed. For the description of an "average" transition region, these assumptions are that :

1. the transition region is homogeneous, plane parallel and an isothermal corona can be appended to it;
2. it is in hydrostatic equilibrium;
3. it is in ionization equilibrium; and
4. it has zero magnetic field or the magnetic field is aligned vertically.

The emergent intensity of a line at a distance ρ from the centre of the disk in a region governed by these assumptions is given by

$$I(\rho)_o = 1.73\times10^{-16}\ gf\ A \int G(T_e) n_e^2 \frac{dh}{\mu}, \quad (4)$$

where $\mu = \sqrt{r^2-(\rho R_o)^2}/r$ for $\rho > 1$,

and ρ is one half this quantity for $\rho < 1$. ρ is measured in units of R_o, the solar radius and is measured from the point where the line-of-sight is closest to the centre of the Sun. The most systematic approach to building models of the 'average' transition region has been based on the Harvard observations from OSO-4 and OSO-6. The approach has been to describe the transition region and the low corona by three model parameters, based on the fact that each ion has a maximum abundance only over a restricted temperature range. Thus, the intensity of a line due to Mg X, which has maximum abundance at 1.2×10^6K, depends mainly on the square of the electron density in the isothermal corona and therefore on the square of the scaled base pressure p. On the other hand, the intensity of a line like O VI, whose abundance maximises at 300,000 K, depends on the temperature gradient or the downward conductive flux F_c. Both intensities depend on the temperature of the isothermal corona T_c. So, in principle, a proper choice of these parameters should be able to predict the observed intensities of lines formed in the transition region and the low corona. Conversely, observations of lines originating from these regions can be used to fix the three parameters.

On the basis of the three parameter model, Withbroe (1970) successfully predicted the center-limb (C-L) variation of a number of lines formed in the T-region. He first fixed T_c, by measuring the ratio of lines formed outside the limb at 1.8×10^6K. Then a scaled pressure of 6×10^{14} ergs cm^{-3} K and a conductive flux of 6×10^5 ergs cm^{-2} sec^{-1} described the mean equatorial chromosphere-corona transition region adequately. However, for four lines formed shortward of the Lyman limit, λ703 of O III, λ630 of O V, λ554 of O IV and λ765 of N IV, the observed C-L curves were flatter at the limb compared to the typically peaked limb brightening curves of the other lines. This flattening could be satisfactorily explained in terms of spicules piercing into the transition region and shielding these radiations.

Fig. 2 shows a more extended set of observation from OSO-6 (Withbroe and Gurman 1973). The observed intensities have been plotted as a function of Mg X intensity. The characteristic temperatures of the ions observed range from $10^{5\cdot3}$ K to $10^{6\cdot55}$ K. The observed Mg X intensity range is from 20 to 2000 ergs cm^{-2} s^{-1} str^{-1}.

For a selected Mg X intensity, intensities of other lines were obtained from the consolidated observations shown in Figure 2 and compared with predicted intensities calculated according to equation (4). The three parameters, p, T_c and F_c were adjusted so that there was over all agreement between the predicted intensities and the observed ones. It is note-worthy that to be able to describe intensities of lines formed over a wide range of temperatures and base pressures, the conductive flux F_c varies as $p^{1\cdot8}$ for log p < 15.6 and is constant at 6×10^6 ergs cm^{-2} s^{-1} for log p > 15.6. Notice also that at log p = 15.6, the observed intensity correlations for N V, O VI and Ne VIII show a marked discontinuity; for Na IX and Al XI this is not prounounced and it is entirely absent for Si XII and Fe XVI. Lines that show the discontinuity clearly, are all formed in the temperature range 10^5 to 10^6 K. Further, at the low intensity side of the discontinuity, the slope of the correlation is markedly less than unity, while it is unity on the high intensity side. Since the lines formed between 10^5 and 10^6 K are the ones that primarily influence the value of $\frac{dT}{dh}$, the changing slopes of the observed intensity correlation should contain information about the way in which F_c varies with height and temperature in the transition region. This would be investigated in detail in a later Section.

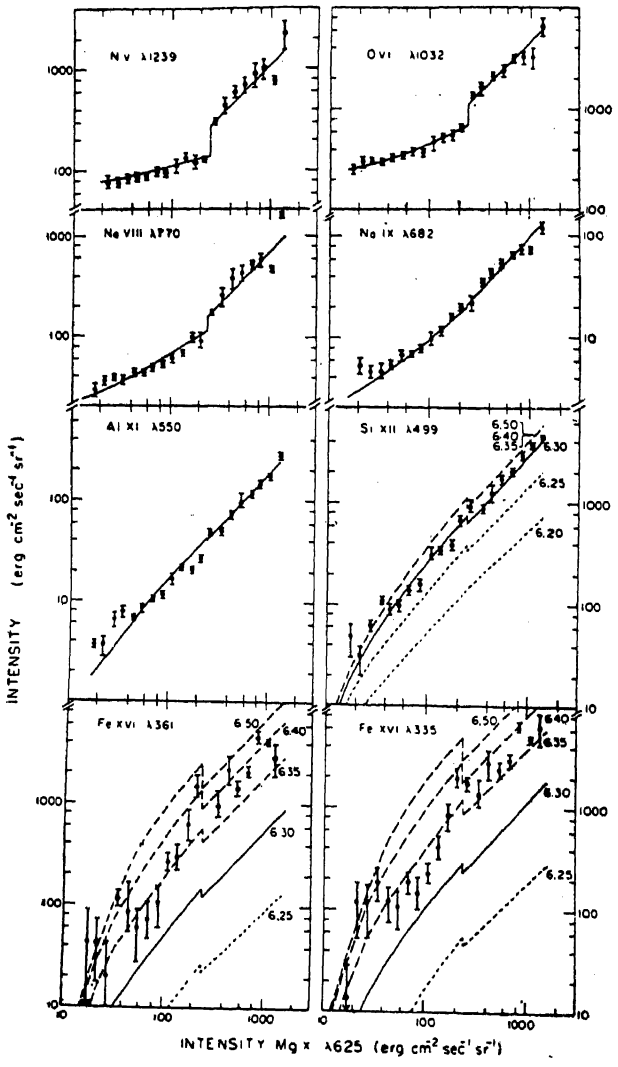

Fig. 2: Observed intensity correlations from OSO-6 data (After Withbroe and Gurman (1973), courtesy. The Astrophysical Journal, The University of Chicago Press).

The model construction approach has successfully provided a zero order approximation of the physical conditions in the transition region. Table 1 summarises these results. However, they do not specify, where the transition region starts. Only indirect evidence, setting the start of the transition region at 2000 km, is available from limb brightening curves of transition region lines having wavelengths shortward of the Lyman limit. Two kinds of observations give a direct estimate of the height at which the transition region starts. Simon and Noyes (1972) used the fact that the position on the disk of any off-centre distinguishable feature would depend on its height of formation. A feature viewed in N V 1239A at 2×10^5 K should be closer to the disk centre than the same feature viewed in Ne VIII 770 A (7×10^5 K), if the two are formed at substantially different heights. Using this technique and high resolution (5" of arc) rocket observations, Simon et al (1975) found that the transition region started definitely below 3000 km (Lyman continuum is assumed to originate around 2000 km). The temperature gradient is steep in this region and begins to

TABLE 1

Model Parameters of the Transition Region—Homogeneous approximation

	'average' quiet region	'average' active region
T_c in 10^6K	1.6—1.8	2.3—2.5
P in 10^{15} $cm^{-3}K$	0.6—0.8	3.0—5.0
F_c in 10^6 ergs $cm^{-2}s^{-1}$	0.6—1.0	4.0—5.0

decrease in the vicinity of 7×10^5 K approximately, at a height of 3500 km. Between 10^5 and $10^{6.4}$K, this geometrical model agrees with the three parameter model. Similar conclusions have been reached by Jordan et al (1973), who interpret the ratio of disk and limb intensities in terms of heights of formation. Again, high resolution rocket spectra fix the beginning of the transition region at 2100 ± 850 km and the steep rise in temperature tapers off around 7×10^5 K. Notice that both geometrical methods are independent of relative abundances, ionization and hydrostatic equilibrium assumptions. Also the presence of inhomogenities does not alter the estimates made.

INHOMOGENEOUS MODELS :

It is now well known that all EUV emission upto a temperature of at least 7×10^5 K exhibit the network structure that is characteristic of the chromosphere. Beyond the transition region, at 1.2×10^6 K, this structure is essentially absent. The most immediate consequence of this horizontal structure is that the conductive flux deduced on the basis of a homogeneous approximation is overestimated. Raghavan (1977) has examined the consequence of this concentration of the measured flux in the network border, on the intensity correlations observed by Withbroe and Gurman (Fig. 2). There are two striking features in these correlations. For all lines formed in the ransition region, there is a discontinuity at a Mg X intensity of 250 ergs cm^{-2} s^{-1} str^{-1}; secondly the *slope* of the log intensity plots, on the low intensity side of this discountinuity is much less than unity. Comparison of the observed slopes with those obtained on the basis of all the measured flux coming from the network borders alone, shows that the fractional emitting area α in any transition region ion depends on the Mg X intensity as follows :

$$\alpha = D\, I_{Mg\,X}^{-k} \quad ; k = 1\text{-}m. \qquad (5)$$

Here D and k are constants for any ion, and m is the observed slope of the intensity correlation. The slope m increases with the increasing temperature of formation of the line ; thus the above relation shows that at a fixed Mg X intensity, the fractional area increases with in-

TABLE 2

Fractional Areas and F_{Mgx} / F_{ion} as a function of temperature

Element	Log T_{max}	k = 1-m	D	α*	$<\alpha>$	B = F_{Mgx}/F_{ion}
N V	5.30	0.78	5.15	0.364	0.315	11.1
O VI	5.50	0.66	3.14	0.330	0.240	5·9
Ne VIII	5.85	0.51	2.69	0.474	0.328	5.8

*Fractional area calculated for a Mg X intensity of 30 ergs $cm^{-2} s^{-1} str^{-1}$

creasing temperature i.e. with increasing height. At a fixed temperature, the fractional emitting area decreases with increasing Mg X intensity i.e. with increasing rate ot coronal heating. Table 2 shows the variation of fractional areas, average fractional areas and the ratio of conductive fluxes, for the three ions emitting in the transition region.

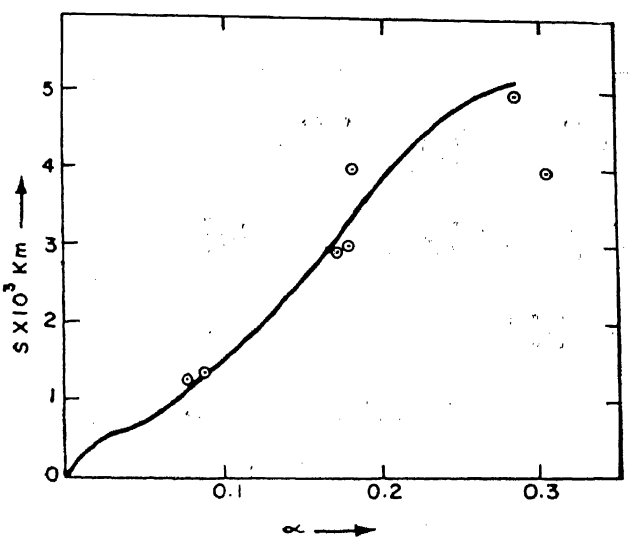

Fig. 3: Variation of the fractional area of cross-section of the magnetic tube of flux with distance along the tube. Circles are fractional areas calculated using Equation (5) and Table 2.

Giovanelli (1975) has considered the heat balance equation in a static transition region, threaded by magnetic lines of force. The area of cross-section of the magnetic flux tube is determined by assuming pressure equlibrium between the inside and outside of the tube. Inside, the gas pressure is assumed to be negligible compared to the magnetic pressure, while outside the pressure is the sum of the turbulent and gas pressures. The heat balance equation is solved for the transition region in which no heat is deposited or generated. It leads to the interesting solution that both the height of the transition region and the temperature of the corona depend on the rate of heating of the corona. The higher the rate of heating, the higher is the coronal temperature and the lower the height of the transition region. Thus, for higher heating rates, a larger heat flux is conducted downward. This is dissipated away by radiation at the higher densities prevailing at lower heights. Comparison of Giovanelli's model of the magnetic tube of flux with the fractional emitting areas deduced by Raghavan is shown in Fig. 3. The agreemet between the two is excellent.

Results from the ATM experiment clearly show the need to use different models for the network border and interior. Mariska and Withbroe (1975) have shown, on the basis of a three parameter model for O VI, that the conductive flux in the border is three times smaller than that inside the network. Using ATM data, Reeves (1976) has come to the conclusion that the coronal temperature above the border and the interior is the same, but the electron density in the interior is somewhat higher. Reeves has also found that the *average* width of the border is not a strong function of temperature, in agreement with analysis of low resolution data (Table 2).

One of the major questions in studying the transition region is the identification of the emission features in the transition region with features on the chromosphere. Brueckner and Bartoe (1974) have identified O IV λ 554 emission with the H α coarse dark mottles. No correlation with the bright mottles is evident. At 5×10^5K (Ne VII λ 465), however, the identification is not exact and the emission comes from a wider area. Withbroe and Mariska (1976) find that the centre-limb variations of C II λ 1335, C III λ 1176, N III λ 991 and O VI λ 1032 can only be explained on the basis of 20% of the emission coming from the transition region sheaths of spicules. The rest comes from features having plane parallel geometry.

It is evident therefore, that the concept of an unique transition regon, like that of an unique coronal temperature is at best an approximation It is becoming increasingly clear that the interface between the chromosphere and the corona is anything but uniform in location and thickness. The term transition region may eventually come to signify only a regime of temperatures between those obtaining in the chromosphere and those in the corona. Future observations would surely unfold all the intersting features of this complex region.

ACKNOWLEDGEMENTS :

It is a pleasure to thank Dr. M.K.V. Bappu for hospitality during a summer visit to the Indian Institute of Astrophysics, Bangalore, where this review was completed.

References :

Athay, R.G. 1966, *Astrophys. J.*, **145,** 784.
Brueckner, G.E. and Bartoe, J.D. 1974, *Solar Phys.*, **38,** 133.
Dupree, A.K. and Goldberg, L. 1967, *Solar Phys.*, **1,** 229,
Giovanelli, R.G. 1975, *Solar Phys.*, **44,** 315.
Jordan, C., Ridgeley, A. and Wilson, R. 1973, *Astron. Ap.* **27,** 101.
Mariska, J.T. and Withbroe, G.L. 1975, *Solar Phys.*, **44,** 55,
Moore, R.L. and Fung, P.C.W. 1972, *Solar Phys.*, **23,** 78.
Pottasch, S.R. 1964, *Space Sci. Rev.*, **3,** 816.
Raghavan, N. 1977, *Solar Phys.*, in press.
Reeves, E.M. 1976, *Solar Phys.*, **46,** 53.
Reimers, D. 1970, *Astron. Ap.*, **10,** 318.
Simon, G.W. and Noyes, R.W. 1972, *Solar Phys.*, **22,**450.
Simon, G.W., Seagraves, P.H., Tousey, R., Purcell J.D. and Noyes, R.W. 1974, *Solar Phys.*, **39,** 121.
Withbroe, G.L. 1970, *Solar Phys.*, **11,** 708.
Withbroe, G.L. and Gurman J.B. 1973, *Astrophys. J.*, **183,** 279.
Withbroe, G.L. and Mariska, J.T. 1976, *Solar Phys.*, **48,** 31.

—— : o : ——